



**HAL**  
open science

## **Thermodynamic characterization of the redox centers in a representative domain of a novel c-type multiheme cytochrome**

Leonor Morgado, Ana P Fernandes, Yuri y Londer, P Raj Pokkuluri, Marianne Schiffer, Carlos A Salgueiro

### ► **To cite this version:**

Leonor Morgado, Ana P Fernandes, Yuri y Londer, P Raj Pokkuluri, Marianne Schiffer, et al.. Thermodynamic characterization of the redox centers in a representative domain of a novel c-type multiheme cytochrome. *Biochemical Journal*, 2009, 420 (3), pp.485-492. <10.1042/BJ20082428>. <hal-00479144>

**HAL Id: hal-00479144**

**<https://hal.science/hal-00479144v1>**

Submitted on 30 Apr 2010

**HAL** is a multi-disciplinary open access archive for the deposit and dissemination of scientific research documents, whether they are published or not. The documents may come from teaching and research institutions in France or abroad, or from public or private research centers.

L'archive ouverte pluridisciplinaire **HAL**, est destinée au dépôt et à la diffusion de documents scientifiques de niveau recherche, publiés ou non, émanant des établissements d'enseignement et de recherche français ou étrangers, des laboratoires publics ou privés.



HAL Authorization

**Thermodynamic characterization of the redox centers in a representative domain of a novel *c*-type multiheme cytochrome**

Leonor Morgado<sup>\*</sup>, Ana P. Fernandes<sup>\*</sup>, Yuri Y. Londer<sup>†2</sup>, P. Raj Pokkuluri<sup>†</sup>, Marianne Schiffer<sup>†</sup>,  
Carlos A. Salgueiro<sup>\*1</sup>

*<sup>\*</sup>Requimte-CQFB, Departamento de Química, Faculdade de Ciências e Tecnologia, Universidade Nova de Lisboa, Campus Caparica, 2829-516 Caparica, Portugal*

*<sup>†</sup>Biosciences Division, Argonne National Laboratory, Argonne, Illinois 60439, USA*

<sup>1</sup>Corresponding author. Departamento de Química, Faculdade de Ciências e Tecnologia, Universidade Nova de Lisboa, Campus Caparica, 2829-516 Caparica, Portugal. Telephone: (+351) 212 948 300. Fax: (+351) 212 948 385. *E-mail address:* csalgueiro@dq.fct.unl.pt

<sup>2</sup>Present address: *New England Biolabs, 240 County Road, Ipswich, MA 01938, USA*

SHORT PAGE HEADING TITLE: “Thermodynamic characterization of a novel *c*-type multiheme cytochrome”

## SYNOPSIS

Multiheme cytochromes that could form protein “nanowires” were identified in *Geobacter sulfurreducens* genome and represent a new type of multiheme cytochromes. The sequences of these proteins, two with 12-hemes (GSU1996, GSU0592) and one with 27-hemes (GSU2210) suggest that they are formed by domains homologous to triheme cytochromes *c*<sub>7</sub>. While all three hemes have bis-His coordination in cytochromes *c*<sub>7</sub>, in each domain of the above polymers the heme equivalent to heme IV has His-Met coordination. We previously determined the structure and measured the macroscopic redox potential of one representative domain (domain C) of a dodecaheme cytochrome (GSU1996). In the present study, the microscopic redox properties of the individual heme groups of domain C were determined using NMR and UV-visible spectroscopies. The reduction potentials of the hemes for the fully reduced and protonated protein are different from each other (heme I, -106 mV; heme III, -136 mV; heme IV, -125 mV) and are strongly modulated by redox-interactions. This result is rather surprising since the His-Met coordinated heme IV does not have the highest potential as was expected. The polypeptide environment of each heme group and the strong heme pairwise redox interactions must play a dominant role in controlling the individual heme potentials. The strong redox interactions between the hemes extend the range of their operating potentials at physiological pH (heme I, -71 mV, heme III, -146 mV and heme IV -110 mV). Such a modulation in heme potentials is likely to have a functional significance in the metabolism of *Geobacter sulfurreducens*.

Keywords: Multiheme, cytochrome *c*, *Geobacter*, axial coordination

Abbreviations: *Gs*, *Geobacter sulfurreducens*; PpcA, *Geobacter sulfurreducens* triheme cytochrome (GSU0612); PpcB *Geobacter sulfurreducens* triheme cytochrome (GSU0364)

Accepted Manuscript

## INTRODUCTION

Microrganisms of the *Geobacteraceae* family have a major role in the dissimilatory reduction of metals and radionuclides coupled to the oxidation of organic matter in soils and sediments [1]. *Geobacter* species are metabolically diverse; in particular, they can use both soluble and insoluble electron acceptors. Especially interesting is the biological reduction of insoluble electron acceptors [2]; since the reduction occurs outside the cell rather than in the periplasm, it requires electron transfer through the outer membrane to the outside of the cell [3, 4]. This electron transfer capability relies on a group of electron transfer proteins, mainly cytochromes *c*, which are abundant in *Geobacteraceae*. Indeed, more than a hundred genes encoding for *c*-type cytochromes were identified in *Geobacter sulfurreducens* (*Gs*) genome [5] and most of them contain multiple hemes. The best studied cytochromes in *Gs* are the periplasmic triheme cytochromes *c*<sub>7</sub>, PpcA and PpcB [6-9]. The family of cytochromes *c*<sub>7</sub> is structurally homologous to the tetraheme cytochromes *c*<sub>3</sub> with heme II deleted [10]. To maintain consistency with the literature, the heme groups in the triheme cytochromes are numbered I, III and IV. In cytochromes *c*<sub>7</sub> and cytochromes *c*<sub>3</sub> all the heme groups have bis-His axial coordination.

*Gs* genome encodes two proteins with 12 heme binding motifs (GSU0592 and GSU1996) and one with 27 heme binding motifs (GSU2210). Homologous dodecaheme cytochromes were identified in the genomes of *Geobacter metallireducens* and *Geobacter uraniireducens*. These proteins represent a new class of multiheme cytochromes. Their sequences suggest a multidomain organization of highly homologous cytochrome *c*<sub>7</sub>-type domains with a mixed type of heme coordination (His-His and His-Met) within each domain [9-11]. The physiological function of these polymers is not known though one of their putative functions is to contribute to the enhancement of the cellular electron-storage capacity. Indeed, by having a large number of redox centers, these molecules, in the absence of external electron acceptors are suggested to allow the continuous flow of electrons from the inner membrane to maintain cellular energy demands until new acceptors can be reached in the environment [12]. The putative structure of the 12-heme cytochrome GSU1996 is a one-dimensional array composed of four triheme cytochrome domains (termed A, B, C and D) covalently bound by short linkers. Each domain of the mature protein GSU1996 was expressed individually in *E. coli* [10]. The crystal structure of the single domain C was determined at 1.7Å resolution together with its macroscopic midpoint potential [10]. Both the structural data and the sequence homology among each of the four domains revealed that each domain has structural features that are unique for multiheme *c*-type cytochromes: two of the hemes (I and III) have bis-His axial coordination while the third one (heme IV) has His-Met axial coordination.

To shed light on the redox properties of the hemes in this new class of multiheme cytochromes isolated from *Gs* we fully characterized the redox properties of the heme groups in the domain C of the dodecaheme cytochrome GSU1996 using NMR and UV-visible spectroscopic techniques. Our study shows that the reduction potentials of the heme groups are different from each other and are strongly modulated by the structure of the protein and by redox interactions that expand the reduction potential working range of the cytochrome. The heme with His-Met axial coordination does not have the highest reduction potential contrary to what is expected.

## EXPERIMENTAL

### Domain C sample preparations

Gs domain C was expressed in *E. coli* and purified as described previously [10]. The buffer used in the purification was exchanged to 20mM NaCl by ultrafiltration methods for all samples. For NMR studies the protein was lyophilized twice with  $^2\text{H}_2\text{O}$  (99.9% atom) and then re-suspended in 600 $\mu\text{l}$  of 80mM phosphate buffer with NaCl (final ionic strength of 250mM) solution prepared in 99.96%  $^2\text{H}_2\text{O}$ . Protein concentration ( $\sim 70\mu\text{M}$  for redox titrations and  $\sim 140\mu\text{M}$  for structural studies) was determined using the specific absorption coefficient of the  $\alpha$ -band of the reduced form for PpcA [13]. The pH was adjusted by the addition of small amounts of  $\text{NaO}^2\text{H}$  or  $^2\text{HCl}$ . The reduced sample was obtained by adding gaseous hydrogen in the presence of catalytic amounts of Fe-hydrogenase isolated from *Desulfovibrio vulgaris* (Hildenborough). The partially oxidized samples, used for NMR redox titrations, were obtained by first removing the hydrogen from the reduced sample with nitrogen and then adding controlled amounts of air into the NMR tubes.

### NMR experiments

All NMR spectra were obtained on a Bruker Avance 600 spectrometer at 288K and were calibrated using the water signal as internal reference. The proton chemical shifts reported are relative to tetramethylsilane. To assign the heme substituents signals in the reduced form,  $^2\text{H}_2\text{O}$  NOESY (50-100ms mixing time) and TOCSY (60ms mixing time) spectra were acquired using standard pulse techniques collecting  $2048(t_2) \times 512(t_1)$  data points to cover a sweep width of 8 kHz, with 64 scans per increment. To map the oxidation of the individual hemes throughout the redox titrations, a series of 2D-exchange spectroscopy (EXSY) experiments were collected for each pH value (covering the range 5.0-8.5) at several degrees of oxidation. All the 2D-EXSY NMR experiments were acquired with a mixing time of 25 ms and recording  $2048(t_2) \times 256(t_1)$  data points to cover a sweep width of 42kHz, with at least 256 scans per increment.

### Ring-current shifts calculation

The heme substituent chemical shifts were calculated by correcting the heme proton reference shifts (9.36 ppm for heme meso protons, 6.13 for heme thioether methines, 3.48 for heme methyls, and 2.12 for heme thioether methyls) [14] with the ring current shifts calculated from the domain C crystal structure, following the procedure described by Turner et al. and Messias et al. [15, 16].

### Redox titrations followed by visible spectroscopy

Redox titrations of domain C using  $10\mu\text{M}$  protein solutions in 80mM phosphate buffer (pH 7 and 8) with NaCl (250mM final ionic strength) were performed inside an anaerobic chamber at 288K as previously described [10], with redox mediators at a final concentration of  $1.5\mu\text{M}$ . The reduced fraction of the proteins was determined by the method described by Paquette et al. [17]. The experiments were performed at least two times, and the reduction potentials were found to be reproducible within  $\pm 5$  mV.

### Overview of the method used

To describe adequately the redox properties of the heme groups in a multiheme protein it is necessary to probe individually the redox behavior of each center. NMR spectroscopy is well suited for this purpose since the proton chemical shift variations for each heme substituent are

proportional to the degree of oxidation of that particular heme [18-20]. When the intermolecular electron transfer rate is slow and the intramolecular electron transfer rate is fast on the NMR timescale, four oxidation stages connected by steps of one electron transfer can be defined each containing the microstates with 0, 1, 2, or 3 oxidized hemes. The heme methyl substituents are the most suitable ones to probe the degree of oxidation of a particular heme because as the protein oxidation progresses, their resonances shift towards empty regions of the NMR spectrum. As previously described, the minimum number of parameters that fully account the redox properties of the centers in a triheme protein is ten [7, 21]. These are the three heme reduction potentials, the deprotonation energy of the protonatable center, three redox interactions between the heme groups (which measure the influence of oxidation stage of one heme on the reduction potential of a neighboring one), and three interactions between the hemes and the protonatable center (redox-Bohr interactions – which account for the pH effect on the heme reduction potentials). Starting from the fully reduced protein (oxidation stage 0), and by following the pH dependence of the heme methyl proton chemical shifts throughout the remaining oxidation stages, the thermodynamic parameters relative to the fully reduced protonated protein can be determined [7, 22]. Given that the NMR data only gives relative parameters, the total protein reduced fractions were measured at pH 7 and 8 using redox titrations followed by visible spectroscopy to determine the absolute values [22]. The experimental uncertainty associated with the NMR data was estimated from the line width of each NMR signal at half height, and the visible data points were given an uncertainty of 3% of the total optical signal.

THIS IS NOT THE VERSION OF RECORD - see doi:10.1042/BJ20082428

Accepted Manuscript

## RESULTS AND DISCUSSION

### Assignment of domain C heme signals in the reduced state

The structure of domain C [10] showed that hemes I and III have bis-histidiny axial coordination (His-His) while heme IV is coordinated by one histidine and one methionine (His-Met) (Figure 1). Thus, as expected, the 1D-<sup>1</sup>H-NMR spectra of domain C, both in the oxidized and reduced forms, are typical of low spin hemes (Figure 2A,B). The protein is diamagnetic when reduced (Fe(II), S=0) and paramagnetic when oxidized (Fe(III), S=1/2). The <sup>1</sup>H-NMR spectrum of the reduced domain C (Figure 2A,B) clearly shows that a methionine residue is an axial heme ligand in solution. The typical pattern of heme axial methionine resonances [23] includes a three-proton intensity peak at approximately -3 ppm, and up to four resolved one-proton intensity peaks in the low-frequency region of the spectrum.

The heme proton resonances in the reduced protein were identified by following the assignment strategy for heme protons in multiheme ferrocycytochromes described by Turner et al. [16] and are indicated in Supplementary Table. This assignment was tested by comparing the observed heme proton chemical shifts with those calculated from the crystal structure. Of the 6 possible permutations for the three sets of heme protons with respect to the crystal structure, one was clearly preferred (*cf.* Supplementary Table and Figure 3) since all three hemes simultaneously had their smallest root mean square deviation (rmsd) from the calculated chemical shifts. The rmsd of the 36 shifts was 0.18 ppm, with deviations of 0.02 (heme I), 0.07 (heme III), 0.09 (heme IV). The shifts correlate very well, even for the protons subject to the larger ring current effects, as it is the case of the protons 10H<sup>I</sup>, 20H<sup>III</sup>, 12<sup>1</sup>CH<sub>3</sub><sup>I</sup>, 2<sup>1</sup>CH<sub>3</sub><sup>III</sup>, 8<sup>2</sup>CH<sub>3</sub><sup>I</sup>, and 8<sup>2</sup>CH<sub>3</sub><sup>IV</sup> (Figure 3; a heme *c* numbered accordingly with IUPAC-IUB nomenclature is indicated in Supplementary Figure). This assignment was further tested by examining the interheme NOE connectivities, measured from the 2D-NOESY spectra, which were then compared with the distances obtained from the crystal structure. All NOE connectivities between protons that are closer than 3 Å were observed in the 2D-NOESY spectra, confirming that both crystal and solution structures are similar.

### Order of oxidation of the heme groups

As mentioned above, the heme groups in domain C are low spin in oxidized and reduced states. This is convenient for NMR studies since widely different well-resolved spectra are obtained for both oxidation states (Figure 2A,B), facilitating the assignment of the heme signals and the determination of their relative order of oxidation. The redox titration of the heme groups followed by 2D-EXSY NMR experiments at pH 8.0 is indicated in Figure 2C-E. These spectra show that domain C exhibits fast intramolecular and slow intermolecular electron exchange on the NMR time scale since signals from a particular heme methyl can be followed throughout the four oxidation stages. The paramagnetic chemical shifts of heme methyl groups 7<sup>1</sup>CH<sub>3</sub><sup>I</sup>, 12<sup>1</sup>CH<sub>3</sub><sup>III</sup>, and 7<sup>1</sup>CH<sub>3</sub><sup>IV</sup> were used to calculate the oxidation fraction of each heme at different stages of oxidation (Table 1). From Table 1 it is possible to obtain the order of oxidation of the hemes: heme III is the heme that becomes more oxidized in the first redox step (stage 1), the largest fractional oxidation of heme IV is obtained by the second step (stage 2), followed by heme I (stage 3). Indeed, in the last step heme I oxidation fraction increases by 59%, whereas hemes III and IV only increase 28% and 17%, respectively. Given that heme I has bis-histidiny axial coordination, this data clearly indicates that the heme with His-Met axial coordination (heme IV) is not the heme with the highest reduction potential. As described in Materials and

Methods section, in order to determine the absolute values for the heme reduction potentials, heme-heme redox interactions, and redox-Bohr interactions, it is necessary to monitor the heme oxidation patterns at different pH values by 2D-EXSY NMR and combine this information with that obtained from the redox titrations followed by visible spectroscopy.

### Mapping the heme redox properties of domain C

The pH dependence of the paramagnetic chemical shifts of each heme methyl group in the pH range 5.0-8.5, and the data obtained for redox titrations followed by visible spectroscopy at pH 7 and 8 were used to monitor the thermodynamic properties of domain C. The fittings of both NMR and visible data are reported in Figures 4 and 5, respectively. The thermodynamic parameters are listed in Table 2. The parameters show that the microscopic reduction potentials of each heme are different: heme III has the lowest redox potential in the reduced and protonated protein (-136 mV), followed by hemes IV (-125 mV) and I (-106 mV). The interaction energy (redox interaction) for each pair of hemes is positive, indicating that the oxidation of a particular heme renders the oxidation of its neighbors more difficult. On the other hand, the interaction energies between the hemes and the acid-base center (redox-Bohr interactions) are negative, i.e. the oxidation of the hemes facilitates the deprotonation of the acid-base center, and vice versa. The observed redox-Bohr effect in the redox titration curves (Figure 5) and the dependence of the heme methyl NMR paramagnetic shifts (Figure 4) are not significant in the physiological pH range, implying that the redox-Bohr interactions are small.

The oxidation profile of the heme groups at pH 7 is shown by solid lines in Figure 6, where oxidized fraction of each heme is plotted against the solution potential. The crossovers between the individual curves clearly indicate that the affinity of each redox center is tuned by the neighboring heme groups. The positive redox interactions between the hemes modulate the affinity of each redox center during the oxidation of the protein such that their apparent midpoint reduction potentials  $E_{app}$  (i.e. the point at which the oxidized and reduced fractions of each heme group are equally populated: -71, -146, -110 mV, respectively for hemes I, III and IV) are different in relation to those for the fully reduced protein (Table 2). This effect can be easily seen by comparing the dashed and the solid lines in Figure 6. The dashed lines were generated considering no redox-interactions between the heme groups, whereas the solid ones were obtained with the thermodynamic parameters listed in Table 2. The effect of the positive redox interactions between the hemes is particularly pronounced on the reduction potentials of hemes I and IV. Indeed, since heme III dominates the first stage of oxidation (where hemes I and IV are mostly reduced), its reduction potential is little affected by the oxidation of hemes I and IV and, consequently, the  $E_{app}$  of heme III (-146 mV) is less affected in relation to that of the fully reduced protein (-136 mV). However, with the subsequent oxidation of the protein, the oxidation fractions of hemes I and IV also increase which lead to a strong modulation of the redox behavior of heme III (see plateau on the heme III redox curve in Figure 6). On the other hand, with the progressive oxidation of hemes I and IV, and since a large fraction of heme III is oxidized, their oxidation curves are also modulated and both  $E_{app}$  values increase significantly in comparison with those of the fully reduced protein (*cf.* dashed lines and solid lines of the respective heme in Figure 6). Consequently, the midpoint reduction potentials separation is extended significantly to 75 mV in comparison with that in the fully reduced protein (30 mV) and is physiologically relevant (compare the  $E_{app}$  values for the dashed and solid lines in Figure 6).

### Origins for the low reduction potential of heme IV (His-Met) in domain C

The core of domain C (see Fig. 1) is formed by three hemes where the Fe-Fe distances between hemes I – III, I – IV and III – IV are 11.4, 17.8, 12.0 Å, respectively ([10], PDB code 1rwj). The solvent exposure of the hemes I, III and IV is 79Å<sup>2</sup>, 173Å<sup>2</sup>, and 167Å<sup>2</sup>, respectively. The surroundings of heme I is more hydrophobic than that of the other hemes. The propionic acids of heme I form hydrogen bonds with the peptide nitrogens of residues 44 and 45; heme III propionic acid forms hydrogen bond with the peptide nitrogen of residue 70; and heme IV propionic acid forms a hydrogen bond with peptide nitrogen of residue Met51 (sixth axial ligand of heme IV) and forms a salt bridge with Arg48 (it was erroneously reported to heme III propionic acid in [10]). In Pokkuluri et al. [10], domain C structure was compared with that of the triheme cytochrome *c*<sub>7</sub> PpcA. It was later discovered [8] that the structure of PpcA was influenced by a deoxycholic acid molecule used for crystallization and, therefore, domain C is compared with PpcB [8] in the present study. The Fe-Fe distances between hemes I – III, I – IV and III – IV in PpcB monomer-A (PDB code, 3bxu) are 11.7, 18.2, 12.6 Å, respectively. The iron to iron distances and also the relative orientations of the heme groups of the two proteins are similar (Fig. 7A). Though the heme core of domain C is like that of PpcB, the protein conformation surrounding the hemes is different as a result of the insertions and deletions in the sequences between the two proteins (Fig. 7B). Thus domain C is similar to *c*<sub>7</sub> cytochromes in size with a conserved three heme core, but they differ in their polypeptide conformation and in the axial coordination of heme IV (the sixth axial ligand for heme IV is indicated in Fig. 7B).

For PpcB only a quantitative macroscopic redox characterization was previously performed [8] in contrast to the present study of domain C. All PpcB hemes have bis-His coordination [8] and we determined the macroscopic reduction potential of PpcB to be -137 mV, which is shifted to lower reduction potential when compared with that determined in this work for domain C ( $E_{app}$  - 103 mV). Based exclusively on these macroscopic values it can be hypothesized that the higher macroscopic potential of domain C is due to the heme that has His-Met coordination (heme IV). However, the detailed microscopic characterization carried out in this work for domain C showed that this is not the case. The individual reduction potential values of the hemes are -71, -146 mV, and -110 mV respectively for hemes I, III and IV at pH 7 clearly showing that the His-Met coordinated heme IV does not have the highest reduction potential. Therefore the origin of higher  $E_{app}$  of domain C is not just due to one heme with His-Met coordination.

It was surprising that heme IV did not have the highest reduction potential in domain C since it was observed that in aqueous solution a His-Met coordinated heme had 150 mV higher reduction potential than a His-His coordinated heme [24]. However, the results obtained in domain C are consistent with the observations of heme potentials in the cytochrome subunit of the photosynthetic reaction center from *Rhodospseudomonas viridis*, where three of the hemes have His-Met coordination and one heme has His-His coordination. Although the heme-heme redox interactions couldn't be experimentally obtained for the cytochrome subunit, the redox studies hinted that the heme with His-His coordination does not have the lowest reduction potential [25, 26]. Voigt and Knapp [27] performed a detailed theoretical study in this cytochrome to show how the heme potential can be tuned by electrostatic interactions of the heme with its protein surroundings and with the neighbouring hemes.

The experimental results obtained in this work for domain C and the theoretical predictions made for the cytochrome subunit of photosynthetic reaction center are in contrast to the results obtained for mutants of a cytochrome  $c_3$  [28]. In the study of cytochrome  $c_3$ , Takayama et al. [28] replaced the native His residues to Met in the sixth axial ligand position of each heme. The measured microscopic reduction potential of the heme with His-Met coordination in two mutants was found to be much higher (about +200 mV) than the corresponding bis-His heme in the native protein. In these mutants only the ligand of a heme was changed within the context of the same polypeptide surrounding reflecting the change in potentials caused only by the ligand exchange.

Our results show that the microscopic reduction potential for the heme with His-Met axial coordination in domain C is lower than another heme with His-His axial coordination, indicating that the polypeptide chain surrounding the heme can be the largest factor in determining the heme reduction potential. The protein fold around the hemes controls the intrinsic reduction potentials [29] by controlling the nature of interactions between the heme and the protein and the solvent exposure of the heme. In addition, the close proximity of the redox centres to each other results in the establishment of strong redox interactions between the closest pairs of hemes (Table 2) which modulate the redox properties of the heme groups during the oxidation of the protein (Figure 6).

### Functional implications of the cooperative redox interaction networks

Multiheme cytochromes with high heme content, such as dodecaheme cytochromes of *Gs*, are thought to work as capacitors that enhance the electron-storage capacity of the bacterial periplasm. This large electron-storage capacity is thought to permit continued electron flow from the inner membrane to the periplasm and thus to generate energy that might be used by *Geobacter* species to move toward zones where external terminal electron acceptors are available, as suggested by Núñez et al. [12]. Our results demonstrate that an important advantage of having the redox centers closely and strategically arranged along the polypeptide chain is to extend the range of the protein working redox potentials allowing it to face different electron acceptors.

**ACKNOWLEDGEMENTS**

Dr. David L. Turner is acknowledged for the conception of the thermodynamic program. We acknowledge LabRMN at FCT-UNL and Rede Nacional de RMN for access to the facilities. Rede Nacional de RMN is supported with funds from FCT, Projecto de Re-equipamento Científico, Portugal.

**FUNDING**

This work was supported by Fundação para a Ciência e a Tecnologia – Portugal [POCI/QUI/60060/2004, PPCDT/QUI/60060/2004] and U.S. Department of Energy's Office of Science, Biological and Environmental Research GENOMICS:GTL – USA [DE-AC02-06CH11357]. L.M. is supported by Fundação para a Ciência e a Tecnologia grant SFRH/BD/37415/2007.

## REFERENCES

- 1 Lloyd, J. R. and Lovley, D. R. (2001) Microbial detoxification of metals and radionuclides. *Curr Opin Biotechnol* **12**, 248-253
- 2 Shi, L., Squier, T. C., Zachara, J. M. and Fredrickson, J. K. (2007) Respiration of metal (hydr)oxides by *Shewanella* and *Geobacter*: a key role for multihaem *c*-type cytochromes. *Mol Microbiol* **65**, 12-20
- 3 Mehta, T., Coppi, M. V., Childers, S. E. and Lovley, D. R. (2005) Outer membrane *c*-type cytochromes required for Fe(III) and Mn(IV) oxide reduction in *Geobacter sulfurreducens*. *Appl Environ Microbiol* **71**, 8634-8641
- 4 Reguera, G., McCarthy, K. D., Mehta, T., Nicoll, J. S., Tuominen, M. T. and Lovley, D. R. (2005) Extracellular electron transfer via microbial nanowires. *Nature* **435**, 1098-1101
- 5 Methé, B. A., Nelson, K. E., Eisen, J. A., Paulsen, I. T., Nelson, W., Heidelberg, J. F., Wu, D., Wu, M., Ward, N., Beanan, M. J., Dodson, R. J., Madupu, R., Brinkac, L. M., Daugherty, S. C., DeBoy, R. T., Durkin, A. S., Gwinn, M., Kolonay, J. F., Sullivan, S. A., Haft, D. H., Selengut, J., Davidsen, T. M., Zafar, N., White, O., Tran, B., Romero, C., Forberger, H. A., Weidman, J., Khouri, H., Feldblyum, T. V., Utterback, T. R., Van Aken, S. E., Lovley, D. R. and Fraser, C. M. (2003) Genome of *Geobacter sulfurreducens*: metal reduction in subsurface environments. *Science* **302**, 1967-1969
- 6 Lloyd, J. R., Leang, C., Hodges Myerson, A. L., Coppi, M. V., Cuifo, S., Methe, B., Sandler, S. J. and Lovley, D. R. (2003) Biochemical and genetic characterization of PpcA, a periplasmic *c*-type cytochrome in *Geobacter sulfurreducens*. *Biochem J* **369**, 153-161
- 7 Pessanha, M., Morgado, L., Louro, R. O., Londer, Y. Y., Pokkuluri, P. R., Schiffer, M. and Salgueiro, C. A. (2006) Thermodynamic characterization of triheme cytochrome PpcA from *Geobacter sulfurreducens*: evidence for a role played in  $e^-/H^+$  energy transduction. *Biochemistry* **45**, 13910-13917
- 8 Morgado, L., Bruix, M., Orshonsky, V., Londer, Y. Y., Duke, N. E., Yang, X., Pokkuluri, P. R., Schiffer, M. and Salgueiro, C. A. (2008) Structural insights into the modulation of the redox properties of two *Geobacter sulfurreducens* homologous triheme cytochromes. *Biochim Biophys Acta* **1777**, 1157-1165
- 9 Pokkuluri, P. R., Londer, Y. Y., Duke, N. E., Long, W. C. and Schiffer, M. (2004) Family of cytochrome *c*<sub>7</sub>-type proteins from *Geobacter sulfurreducens*: structure of one cytochrome *c*<sub>7</sub> at 1.45 Å resolution. *Biochemistry* **43**, 849-859
- 10 Pokkuluri, P. R., Londer, Y. Y., Duke, N. E., Erickson, J., Pessanha, M., Salgueiro, C. A. and Schiffer, M. (2004) Structure of a novel *c*<sub>7</sub>-type three-heme cytochrome domain from a multidomain cytochrome *c* polymer. *Protein Sci* **13**, 1684-1692
- 11 Londer, Y. Y., Pokkuluri, P. R., Orshonsky, V., Orshonsky, L. and Schiffer, M. (2006) Heterologous expression of dodecaheme "nanowire" cytochromes *c* from *Geobacter sulfurreducens*. *Protein Expr Purif* **47**, 241-248
- 12 Esteve-Núñez, A., Sosnik, J., Visconti, P. and Lovley, D. R. (2008) Fluorescent properties of *c*-type cytochromes reveal their potential role as an extracytoplasmic electron sink in *Geobacter sulfurreducens*. *Environ Microbiol* **10**, 497-505
- 13 Seeliger, S., Cord-Ruwisch, R. and Schink, B. (1998) A periplasmic and extracellular *c*-type cytochrome of *Geobacter sulfurreducens* acts as a ferric iron reductase and as an electron carrier to other acceptors or to partner bacteria. *J Bacteriol* **180**, 3686-3691

- 14 Pessanha, M., Londer, Y. Y., Long, W. C., Erickson, J., Pokkuluri, P. R., Schiffer, M. and Salgueiro, C. A. (2004) Redox characterization of *Geobacter sulfurreducens* cytochrome *c*<sub>7</sub>: physiological relevance of the conserved residue F15 probed by site-specific mutagenesis. *Biochemistry* **43**, 9909-9917
- 15 Messias, A. C., Kastrau, D. H., Costa, H. S., LeGall, J., Turner, D. L., Santos, H. and Xavier, A. V. (1998) Solution structure of *Desulfovibrio vulgaris* (Hildenborough) ferrocyclochrome *c*<sub>3</sub>: structural basis for functional cooperativity. *J Mol Biol* **281**, 719-739
- 16 Turner, D. L., Salgueiro, C. A., LeGall, J. and Xavier, A. V. (1992) Structural studies of *Desulfovibrio vulgaris* ferrocyclochrome *c*<sub>3</sub> by two-dimensional NMR. *Eur J Biochem* **210**, 931-936
- 17 Paquete, C. M., Turner, D. L., Louro, R. O., Xavier, A. V. and Catarino, T. (2007) Thermodynamic and kinetic characterisation of individual haems in multicentre cytochromes *c*<sub>3</sub>. *Biochim Biophys Acta* **1767**, 1169-1179
- 18 Santos, H., Moura, J. J., Moura, I., LeGall, J. and Xavier, A. V. (1984) NMR studies of electron transfer mechanisms in a protein with interacting redox centres: *Desulfovibrio gigas* cytochrome *c*<sub>3</sub>. *Eur J Biochem* **141**, 283-296
- 19 Salgueiro, C. A., Turner, D. L., Santos, H., LeGall, J. and Xavier, A. V. (1992) Assignment of the redox potentials to the four haems in *Desulfovibrio vulgaris* cytochrome *c*<sub>3</sub> by 2D-NMR. *FEBS Lett* **314**, 155-158
- 20 Santos, H., Turner, D. L., Xavier, A. V. and LeGall, J. (1984) Two-dimensional NMR studies of electron transfer in cytochrome *c*<sub>3</sub>. *Journal of Magnetic Resonance* **59**, 177-180
- 21 Correia, I. J., Paquete, C. M., Louro, R. O., Catarino, T., Turner, D. L. and Xavier, A. V. (2002) Thermodynamic and kinetic characterization of trihaem cytochrome *c*<sub>3</sub> from *Desulfuromonas acetoxidans*. *Eur J Biochem* **269**, 5722-5730
- 22 Turner, D. L., Salgueiro, C. A., Catarino, T., Legall, J. and Xavier, A. V. (1996) NMR studies of cooperativity in the tetrahaem cytochrome *c*<sub>3</sub> from *Desulfovibrio vulgaris*. *Eur J Biochem* **241**, 723-731
- 23 McDonald, C. C., Phillips, W. D. and Vinogradov, S. N. (1969) Proton magnetic resonance evidence for methionine-iron coordination in mammalian-type ferrocyclochrome *c*. *Biochem Biophys Res Commun* **36**, 442-449
- 24 Battistuzzi, G., Borsari, M., Cowan, J. A., Ranieri, A. and Sola, M. (2002) Control of cytochrome *c* redox potential: axial ligation and protein environment effects. *J Am Chem Soc* **124**, 5315-5324
- 25 Dracheva, S. M., Drachev, L. A., Konstantinov, A. A., Semenov, A., Skulachev, V. P., Arutjunjan, A. M., Shuvalov, V. A. and Zaberezhnaya, S. M. (1988) Electrogenic steps in the redox reactions catalyzed by photosynthetic reaction-centre complex from *Rhodospseudomonas viridis*. *Eur J Biochem* **171**, 253-264
- 26 Fritsch, G., Buchanan, S. and Michel, H. (1989) Assignment of cytochrome hemes in crystallized reaction centers from *Rhodospseudomonas viridis*. *Biochimica et Biophysica Acta* **977**, 157-162
- 27 Voigt, P. and Knapp, E. W. (2003) Tuning heme redox potentials in the cytochrome *c* subunit of photosynthetic reaction centers. *J Biol Chem* **278**, 51993-52001
- 28 Takayama, Y., Werbeck, N. D., Komori, H., Morita, K., Ozawa, K., Higuchi, Y. and Akutsu, H. (2008) Strategic roles of axial histidines in structure formation and redox regulation of tetraheme cytochrome *c*<sub>3</sub>. *Biochemistry* **47**, 9405-9415

- 29 Zheng, Z. and Gunner, M. R. (2008) Analysis of the electrochemistry of hemes with  $E_m$ s spanning 800 mV. *Proteins, in press*

Accepted Manuscript

THIS IS NOT THE VERSION OF RECORD - see doi:10.1042/BJ20082428

**Table 1. Redox-dependent heme methyl chemical shifts in domain C at pH 8.0.**

The heme methyls  $7^1\text{CH}_3^{\text{I}}$ ,  $12^1\text{CH}_3^{\text{III}}$  and  $7^1\text{CH}_3^{\text{IV}}$  were chosen to monitor each heme oxidation through the four-oxidation stages (see text). The heme fractions of oxidation,  $x_i$ , in each stage of oxidation were calculated accordingly to the equation  $x_i = (\delta_i - \delta_0) / (\delta_3 - \delta_0)$ , where  $\delta_i$ ,  $\delta_0$ , and  $\delta_3$  are the observed chemical shifts of the heme methyl in stage  $i$ , 0, and 3, respectively.

| Oxidation stage | Chemical shift (ppm) |       |       | $x_i$ |      |      | $\Sigma x_i$ |
|-----------------|----------------------|-------|-------|-------|------|------|--------------|
|                 | I                    | III   | IV    | I     | III  | IV   |              |
| 0               | 3.44                 | 3.86  | 3.62  | 0     | 0    | 0    | 0            |
| 1               | 5.61                 | 24.06 | 11.54 | 0.08  | 0.64 | 0.25 | 0.97         |
| 2               | 14.79                | 26.57 | 30.08 | 0.41  | 0.72 | 0.83 | 1.96         |
| 3               | 31.05                | 35.38 | 35.41 | 1     | 1    | 1    | 3            |

**Table 2. Thermodynamic parameters determined for domain C.**

Diagonal terms (in bold) represent the oxidation energies of the three hemes and the deprotonating energies for the protonatable center in the fully reduced and protonated protein. The off-diagonal elements represent the redox and redox-Bohr interactions energies between the four centers. Standard errors are given in parenthesis.

| Energies (meV)      |                 |                 |                 |                     |
|---------------------|-----------------|-----------------|-----------------|---------------------|
|                     | Heme I          | Heme III        | Heme IV         | Protonatable center |
| Heme I              | <b>-106 (2)</b> | 44 (2)          | 7 (2)           | -4 (6)              |
| Heme III            |                 | <b>-136 (2)</b> | 40 (2)          | -25 (6)             |
| Heme IV             |                 |                 | <b>-125 (2)</b> | -13 (7)             |
| Protonatable center |                 |                 |                 | <b>340 (11)</b>     |

**Figure 1. Structure of domain C [10].**

Heme axial ligands are shown in black: H23 and H36 (Heme I), H26 and H64 (Heme III), M51 and H80 (Heme IV).

**Figure 2. Domain C 1D and 2D NMR spectra.**

(A-B) Lower field regions of the 1D-NMR proton spectra of domain C in the reduced (upper spectrum) and oxidized (lower spectrum) forms. Arrows indicate the protons of the heme axial methionine. (C-E) Portion of 2D-EXSY NMR spectra of partially oxidized domain C. Cross peaks connecting the signals of the heme methyls belonging to hemes I, III, and IV in the different oxidation stages are indicated by dotted, dashed and solid lines, respectively. The cross-peaks connecting different oxidation stages (0-3) are boxed. The Roman and Arabic numbers indicate the heme groups and the oxidation stages, respectively. All spectra were obtained at 288K and pH 8.

**Figure 3. Comparison between the calculated and observed chemical shifts for all heme substituents of reduced domain C.**

The heme substituents of heme I, III, and IV are represented by squares, triangles and circles, respectively. The solid line has a unit slope.

**Figure 4. pH dependence of the  $^1\text{H}$  NMR chemical shift of one heme methyl from each of the three hemes ( $7^1\text{CH}_3^{\text{I}}$ ,  $12^1\text{CH}_3^{\text{III}}$ , and  $7^1\text{CH}_3^{\text{IV}}$ ) of domain C.**

Stages of oxidation 1-3 are represented by the symbols: stage 1 ( $\Delta$ ); stage 2 ( $\square$ ); stage 3 ( $\circ$ ). The full lines represent the best fit of the data using the parameters reported in Table 2. The chemical shift of the heme methyl groups in the fully reduced stage 0 are not plotted since they are unaffected by the pH.

**Figure 5. Domain C redox titrations followed by visible spectroscopy.**

Experiments were performed at 288K at pH 7 (circles) and pH 8 (squares). The solid lines represent the best fit of the experimental data using the parameters reported in Table 2.

**Figure 6. Oxidized fractions of the individual hemes of domain C at pH 7.**

Solid lines were calculated as a function of the solution reduction potential using the parameters reported in Table 2. The dashed lines were generated assuming that no redox interactions exist between each pair of hemes. The arrow indicates, from the left to the right, the  $E_{app}$  values of each heme (the point at which the oxidized and reduced fractions are equally populated). For both solid and dashed lines the order of the  $E_{app}$  values is the same:  $E_{app}^{\text{III}} < E_{app}^{\text{IV}} < E_{app}^{\text{I}}$ .  $\Delta E_{app}$  correspond to the  $E_{app}$  separation between hemes I and III for each set of lines.

**Figure 7. Comparison of domain C and PpcB.**

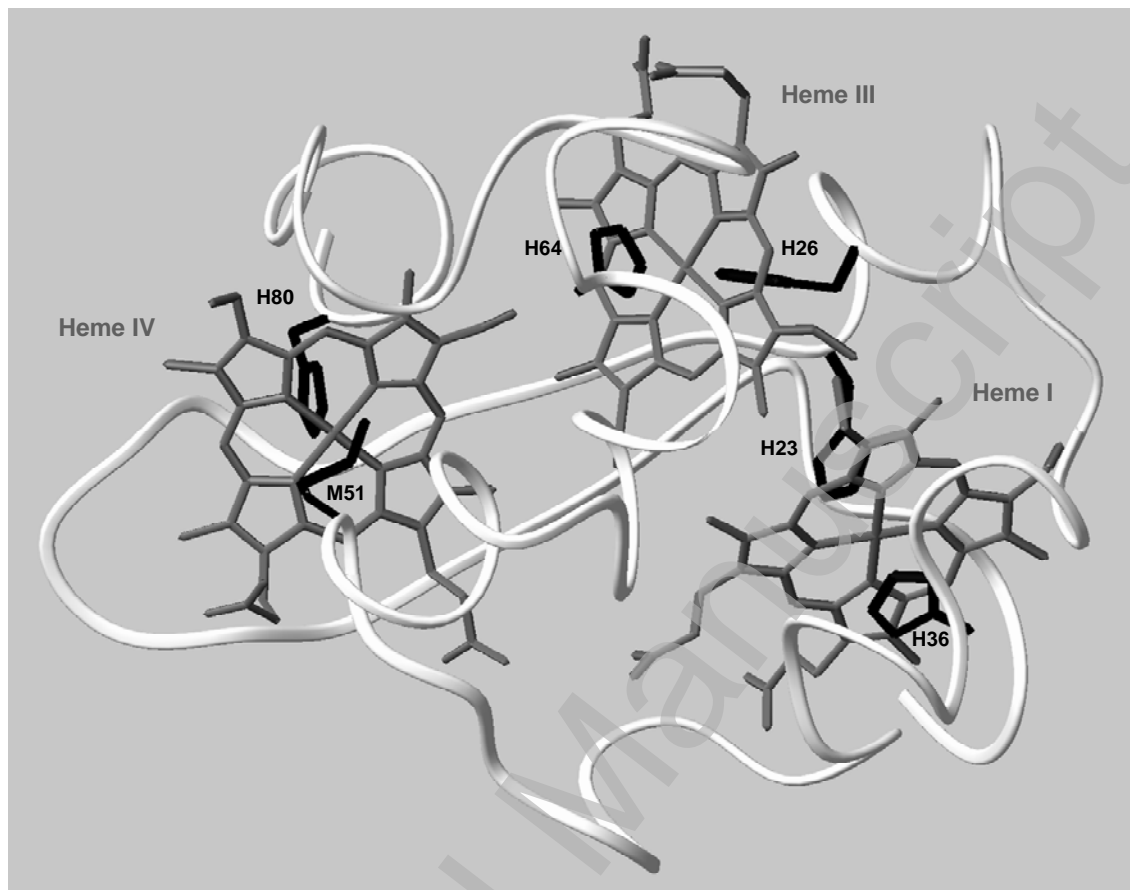
(A) Heme core architecture of domain C [10] (black) and PpcB [10] (grey). The two structures were overlapped with all three heme ring atoms. (B) Structure-guided alignment of the amino acid sequences of domain C of the four domain poly- $c_7$ -type cytochrome GSU1996 and cytochrome  $c_7$  PpcB (monomer A) from *G. sulfurreducens*. Identical residues are shown in bold; the heme binding motif is indicated by the corresponding heme shown below. The sixth axial

ligand to heme IV in both proteins is shown in a grey box (note that these residues do not align in sequence).

Accepted Manuscript

THIS IS NOT THE VERSION OF RECORD - see doi:10.1042/BJ20082428

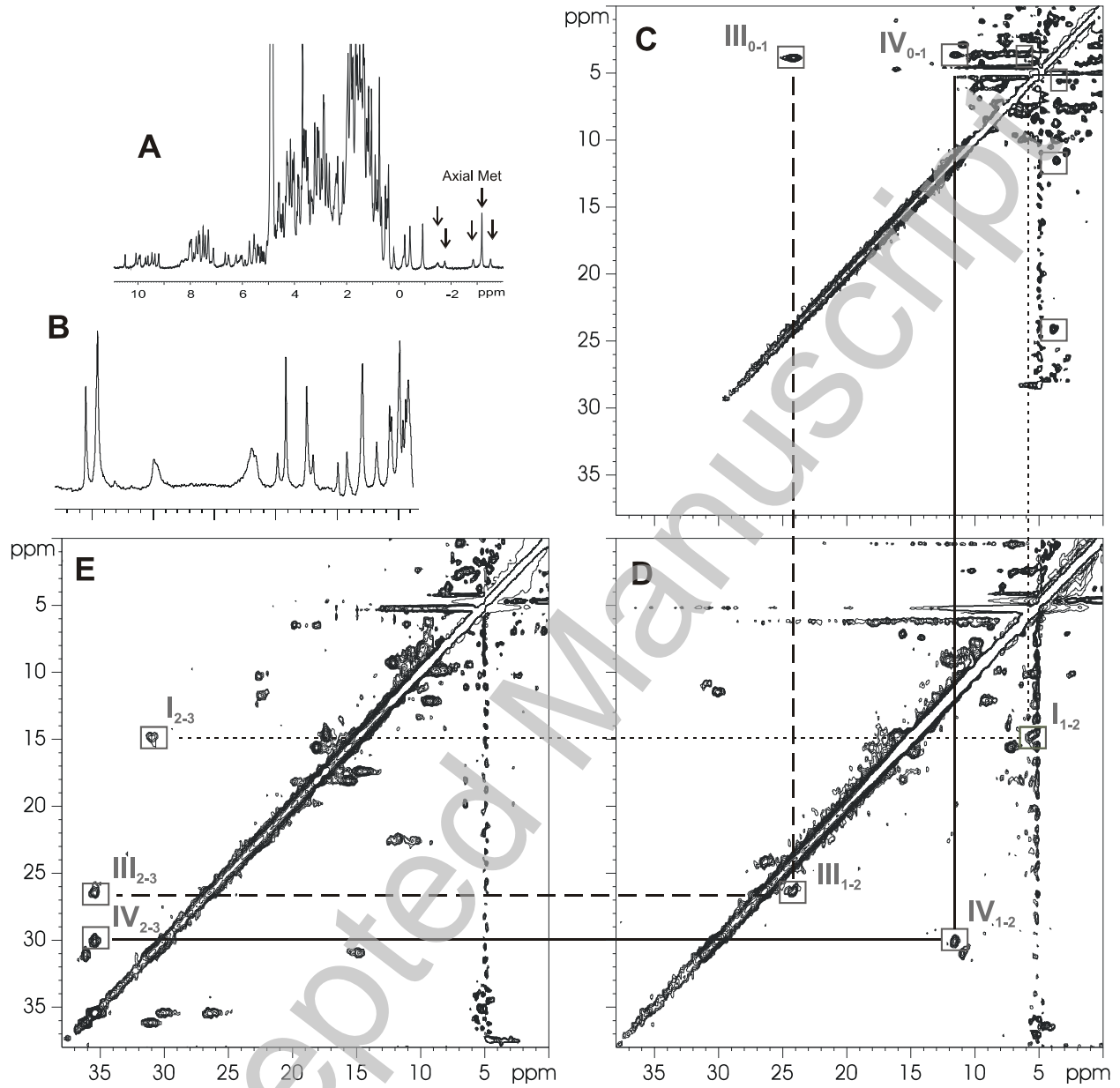
Figure 1



THIS IS NOT THE VERSION OF RECORD - see doi:10.1042/BJ20082428

Accepted

**Figure 2**



THIS IS NOT THE VERSION OF RECORD - see doi:10.1042/BJ20082428

Accepted Manuscript

Figure 3

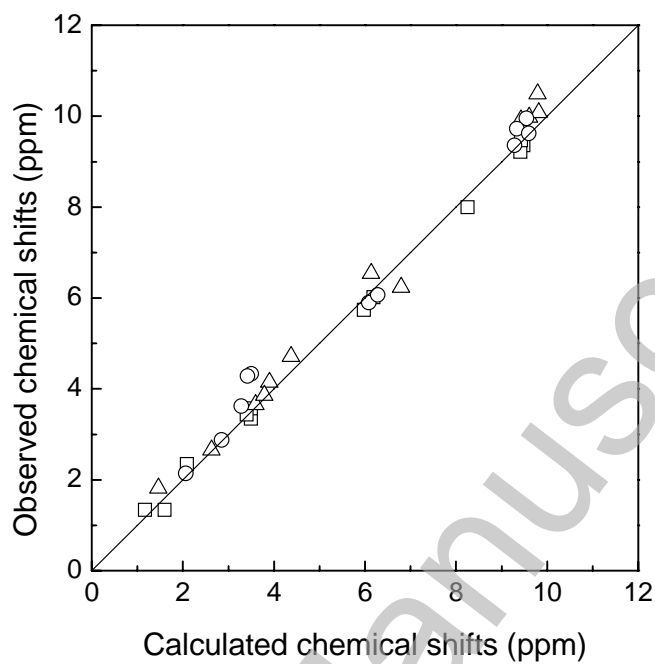
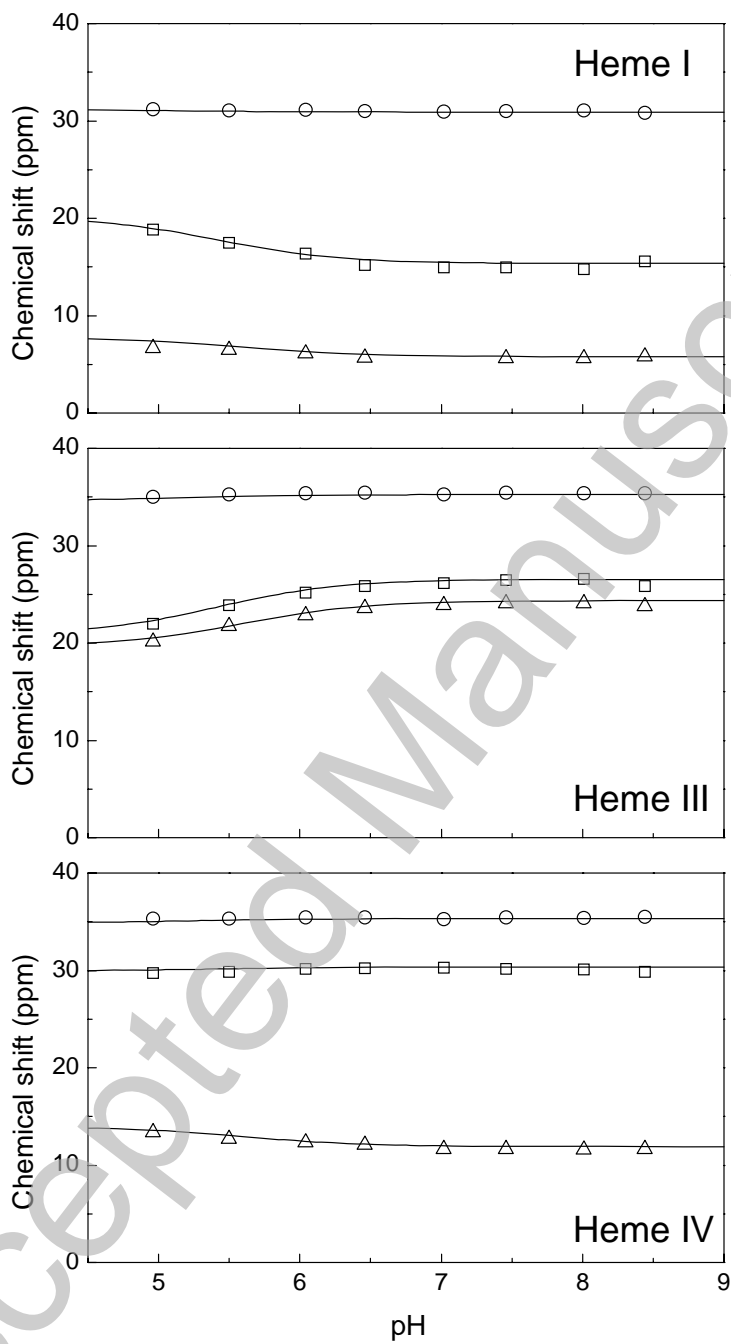


Figure 4



THIS IS NOT THE VERSION OF RECORD - see doi:10.1042/BJ20082428

Accepted Manuscript

Figure 5

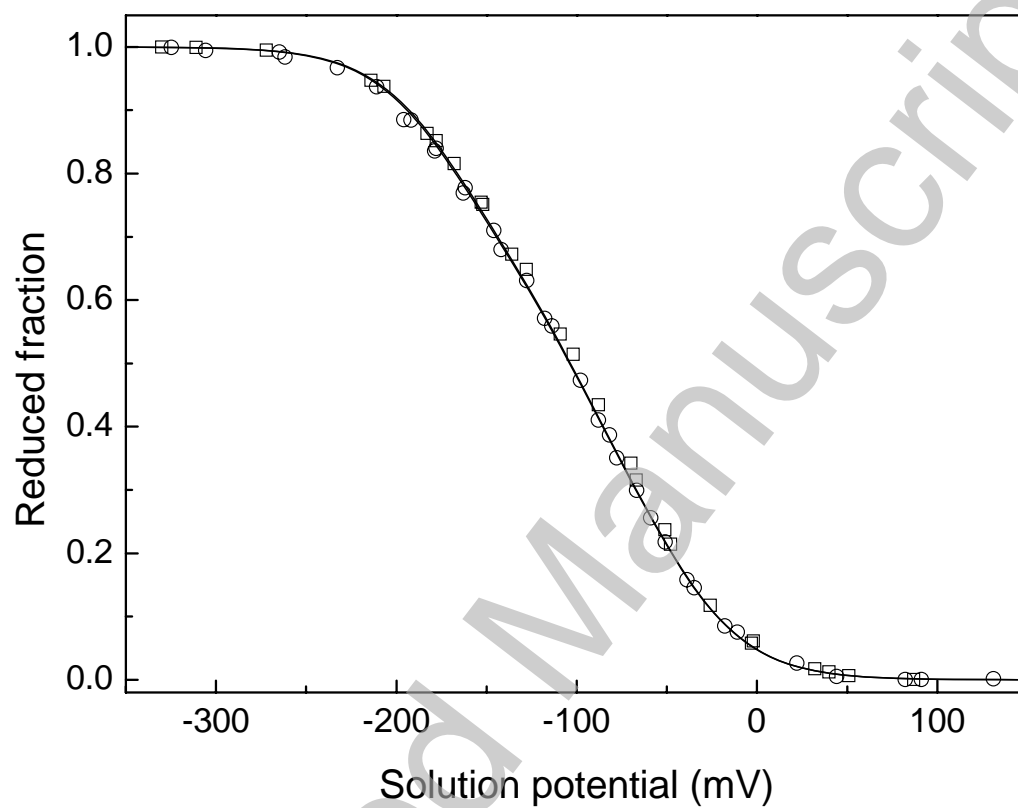


Figure 6

